She4p/Dim1p Interacts with the Motor Domain of Unconventional Myosins in the Budding Yeast, *Saccharomyces cerevisiae*

Hirofumi Toi,*‡ Konomi Fujimura-Kamada,* Kenji Irie,† Yoshimi Takai,† Satoru Todo,‡ and Kazuma Tanaka*§

*Division of Molecular Interaction, Institute for Genetic Medicine, Hokkaido University Graduate School of Medicine, Hokkaido 060-0815, Japan; †Department of Molecular Biology and Biochemistry, Osaka University Graduate School of Medicine, Osaka 565-0871, Japan; and ‡Department of General Surgery, Hokkaido University Graduate School of Medicine, Hokkaido 060-8638, Japan

She4p/Dim1p, a member of the *U*NC-45/*C*RO1/*S*he4p (UCS) domain-containing protein family, is required for endocytosis, polarization of actin cytoskeleton, and polarization of *ASH1* mRNA in *Saccharomyces cerevisiae*. We show herein that She4p/Dim1p is involved in endocytosis and actin polarization through interactions with the type I myosins Myo3p and Myo5p. Two-hybrid and biochemical experiments showed that She4p/Dim1p interacts with the motor domain of Myo3/5p through its UCS domain. She4p/Dim1p was required for Myo5p localization to cortical patch-like structures. Using random mutagenesis of the motor region of *MYO5*, we identified four independent dominant point mutations that suppress the temperature-sensitive growth phenotype of the *she4/dim1* null mutant. All of the amino acid substitutions caused by these mutations, V164I, N168I, N209S, and K377M, could suppress the defects of endocytosis and actin polarization of the *she4/dim1* mutant as well. She4p/Dim1p also showed two-hybrid interactions with the motor domain of a type II myosin Myo1p and type V myosins Myo2p and Myo4p, and was required for proper localization of Myo4p, which regulates polarization of *ASH1* mRNA. Our results suggest that She4p/Dim1p is required for structural integrity or regulation of the motor domain of unconventional myosins.

INTRODUCTION

Endocytosis, the internalization of portions of the plasma membrane along with extracellular fluid, is a universal process performed by all eukaryotic cells. In the budding yeast, *S. cerevisiae*, genetic analysis has identified a link between endocytosis and the actin cytoskeleton (Geli and Riezman, 1998; Wendland *et al.*, 1998). During bud growth, yeast cells show polarized organization of two actin filament-containing structures: cortical actin patches and actin cables (Adams and Pringle, 1984; Kilmartin and Adams, 1984). The formation or reorganization of cortical actin patches is regulated by cortical patch-like protein structures that include Sla1p,

Sla2p, Abp1p, Sac6p (fimbrin), Las17p/Bee1p (a homolog of mammalian Wiskott-Aldrich syndrome protein), Vrp1p (verprolin, a homolog of mammalian Wiskott-Aldrich syndrome protein-interacting protein), Myo3p/Myo5p (type I myosins), Rvs167p (amphiphysin), and proteins of the Arp2/3 complex (Pruyne and Bretscher, 2000). These proteins are involved in the uptake step of endocytosis through actin cytoskeleton regulation (Geli and Riezman, 1998; Wendland *et al.*, 1998).

The *DIM1* gene was isolated in a fluorescence-activated cell sorting-based screen using the fluorescent lipophilic dye FM4-64 to search for factors involved in membrane lipid endocytosis (Wendland *et al.*, 1996). Molecular cloning revealed that *DIM1* was identical to *SHE4* (Wendland *et al.*, 1996; see below). At 38°C, *she4* null mutation (*she4Δ*) results in a two- to threefold reduction in the kinetics of mating pheromone internalization relative to that observed in *she4Δ* cells at 26°C or in wild-type cells (Wendland *et al.*, 1996). Like many endocytosis mutants, *she4Δ* cells show a temperature-sensitive growth defect and a depolarized distribution of actin patches (Wendland *et al.*, 1996; Wendland *et al.*, 1998).

The *SHE4* gene was also identified in an independent screen for factors required for *Swi5p*-dependent *HO* expression. In the same screen, four other genes were identified: *MYO4/SHE1* (type V myosin), *SHE2*, *SHE3*, and *BNI1/SHE5* (Jansen *et al.*, 1996). The *SHE* genes are required for polarized distribution, to daughter cells, of *ASH1* mRNA, which codes for Ash1p, the transcriptional repressor of the *HO* gene (Sil and Herskowitz, 1996; Long *et al.*, 1997; Takizawa *et al.*, 1997). The asymmetric localization of *ASH1* mRNA to daughter cells results in the preferential accumulation of Ash1p in daughter cell nuclei and the selective expression of the *HO* endonuclease in mother cells (Bobola *et al.*, 1996; Sil and Herskowitz, 1996; Long *et al.*, 1997). Myo4p/She1p, She2p, and She3p are proposed to form a complex with *ASH1* mRNA and to be translocated to the bud by the motor activity of Myo4p/She1p (Munchow *et al.*, 1999; Bohl *et al.*, 2000; Long *et al.*, 2000; Takizawa and Vale, 2000). *SHE4* has been shown to be required both for endocytosis and for polarization of *ASH1* mRNA distribution, but the molecular mechanisms by which it influences these events have not been well understood.

The C-terminal half of She4p has significant similarity to *Caenorhabditis elegans* UNC-45, *Podospora anserina* CRO1, and *Schizosaccharomyces pombe* Rng3p (Barral *et al.*, 1998; Berteaux-Lecellier *et al.*, 1998; Wong *et al.*, 2000). This C-terminal conserved region is referred to as the *UNC-45/CRO1/She4p* (USC) domain, and these proteins form the UCS protein family. UNC-45 is specifically expressed in muscle tissues and colocalizes with a specific isoform of myosin heavy chain, where it is proposed to play a role in the assembly of skeletal muscle myosin (Venolia and Waterston, 1990; Barral *et al.*, 1998; Ao and Pilgrim, 2000). Recently, it was reported that UNC-45 acts as a molecular chaperone for the muscle myosin motor (Barral *et al.*, 2002). CRO1 is essential for the transition between the syncytial and cellular stages (Berteaux-Lecellier *et al.*, 1998). Rng3p is required for cytokinesis, and *rng3* genetically interacts with type II myosin, *myo2* (Balasubramanian *et al.*, 1998; Wong *et al.*, 2000).

Myosins are molecular motors that convert the energy of ATP hydrolysis into mechanical work, in the form of translocation along actin filaments. They constitute a large superfamily of proteins implicated in diverse cellular functions (Mooseker and Cheney, 1995; Sellers, 1999). Budding yeast contains a total of five myosins from three types: two type I myosins (*MYO3* and *MYO5*), one type II myosin (*MYO1*), and two type V myosins (*MYO2* and *MYO4*) (Brown, 1997). Conventional (type II) myosins were the first type to be described. They include muscle myosins and similar myosins from nonmuscle cells. They have a two-headed structure and self-associate to form filaments. *MYO1* is implicated in actin-ring formation during cytokinesis and is thought to deliver components required for cell separation to the septum (Watts *et al.*, 1987; Rodriguez and Paterson, 1990; Bi *et al.*, 1998; Lippincott and Li, 1998). Unconventional myosins are either two-headed or single-headed, and, in contrast with conventional myosins, do not seem to form filaments. *MYO3* and *MYO5* have been shown to play an important role in endocytosis and polarized assembly of cortical actin patches (Geli and Riezman, 1996; Goodson *et al.*, 1996). Although deletion of either *MYO3* or *MYO5* does not result in an obvious growth phenotype, a double knockout is synthetically lethal or nearly so, suggesting functional

redundancy between these genes (Geli and Riezman, 1996; Goodson *et al.*, 1996). *MYO2* is thought to be required for polarized growth and transport of certain secretory vesicles along actin cables from the mother to the bud (Johnston *et al.*, 1991; Schott *et al.*, 2002). *MYO4/SHE1* controls the segregation of *ASH1* mRNA as stated above.

In this article, we report that defects in endocytosis and actin cytoskeletal polarization in *she4* mutant are caused by dysfunctions of Myo3/5p. The UCS domain of She4p physically interacts with the motor domain of Myo3/5p, and novel dominant point mutations in the motor region of *MYO5* can bypass the requirement of She4p. She4p also interacts with Myo1p, Myo2p, and Myo4p in two-hybrid assays and is required for proper localization of Myo4p. Our results suggest that the UCS proteins play an important role for proper function of the unconventional, in addition to the conventional, myosins.

MATERIALS AND METHODS

Strains, Media, and Plasmids

The yeast strains used in this study are listed in Table 1. Isolation of temperature-sensitive *myo5* tail mutants will be described elsewhere. The *she4*, *myo3*, *myo5*, *bni1*, and *cla4* disruption; *SHE4*, *MYO1*, and *MYO4* chromosomal green fluorescent protein (GFP) tagging; and *MYO5* chromosomal TAP tagging were carried out using polymerase chain reaction (PCR)-based methods as described previously (Longtine *et al.*, 1998; Rigaut *et al.*, 1999). The *sla2* disruption and *MYO2* GFP-tagged strains were constructed on our strain background as follows. The regions containing the disruption or tagging marker and the flanking sequences were PCR amplified using either DDY546 (*sla2Δ1::URA3*) or YJC1431 (*MYO2-GFP::HIS3*) genomic DNA as a template. The resulting DNA fragment was then introduced into YEF473. Unless otherwise specified, strains were grown in YPDA-rich medium (1% yeast extract [Difco, Detroit, MI], 2% bacto-peptone [Difco], 2% glucose, and 0.01% adenine). Strains carrying plasmids were selected in synthetic medium (SD) containing the required nutritional supplements (Sherman, 1991). When indicated, 0.5% casamino acids (Difco) were added to SD medium without uracil (SDA-Ura). The plasmids used in this study are listed in Table 2. Schemes for the construction of plasmids and the sequences of PCR primers are available upon request. *Escherichia coli* strains DH5α and XL1-Blue were used for the construction and amplification of plasmids. Yeast transformations were performed using the lithium acetate method (Elble, 1992; Agatep *et al.*, 1998).

Two-Hybrid Screening

Two-hybrid screening was performed as described previously (Bartel *et al.*, 1993). L40 cells, carrying pKT1286, was independently transformed with three yeast genomic DNA libraries (Y2HL-C1, -C2, and -C3) (James *et al.*, 1996), incubated in SD-Trp-Leu medium overnight, and then plated on SD-Trp-Leu-His plates supplemented with 1 mM 3-aminotriazole. Approximately 1.2×10^5 transformants were screened for each library. After incubation for several days at 30°C, 120, 1, and 120 colonies were picked up from the Y2HL-C1, -C2, and -C3 transformants, respectively. From these clones, 13 plasmids were isolated and reintroduced into L40 cells carrying pKT1286 to retest for growth on SD-Trp-Leu-His + 1 mM 3-aminotriazole plates. All 13 clones showed positive interactions and were then sequenced. Type I myosins, *MYO3* (six clones) and *MYO5* (six clones), and a transcriptional factor, *ABF1* (1 clone), were obtained. Because most of clones analyzed encoded type I myosins, other clones were not analyzed further. Quantification of β-galactosidase activity was performed using *o*-nitrophenyl β-D-galactopyranoside

Table 1. The yeast strains used in this study

Strain[a]	Genotype	Origin/Reference
L40	*MAT**a** lys2-801 his3Δ-200 trp1-901 leu2-3,112 ade2 LYS2::(lexAop)₄-HIS3 URA3::(lexAop)₈-lacZ*	Hollenberg *et al.*, 1995
TAT7[b]	*MAT**a** lys2-801 his3Δ-200 trp1-901 leu2-3,112 ade2 LYS2::(lexAop)₄-HIS3 ura3::(lexAop)₈-lacZ*	Imamura *et al.*, 1997
YKT550[b]	*MAT**a** lys2-801 his3Δ-200 trp1-901 leu2-3,112 ade2 LYS2::(lexAop)₄-HIS3 URA3::(lexAop)₈-lacZ she4Δ::KanMX6*	This study
YEF473	*MAT**a**/α lys2-801/lys2-801ura3-52/ura3-52 his3Δ-200/his3Δ-200 trp1Δ-63/trp1Δ-63 leu2Δ-1/leu2Δ-1*	Longtine *et al.*, 1998
YKT159	*MAT**a** myo3Δ::TRP1 MYO5-EGFP::KanMX6*	This study
YKT288	*MAT**a** myo3Δ::TRP1 MYO5-EGFP::KanMX6 she4Δ::HIS3MX6*	This study
YKT114	*MAT**a** myo3Δ::TRP1 myo5Δ::HIS3MX6*	This study
YKT274	*MAT**a**/α SHE4-EGFP::KanMX6/SHE4*	This study
YKT275	*MAT**a** she4Δ::HIS3MX6*	This study
YKT276	*MATα she4Δ::HIS3MX6*	This study
DDY322	*MATα ura3-52 his3Δ-200 leu2-3,112 abp1Δ::LEU2*	A gift from Dr. Drubin
DDY1520	*MAT**a** ura3-52 his3Δ-200 trp1Δ-63 leu2Δ-1 aip1Δ::URA3*	A gift from Dr. Drubin
YMW211U	*MAT**a** lys2-801 ura3-52 his3Δ-200 trp1Δ-63 leu2-1 arp2-1(H330L)::URA3*	Madania *et al.*, 1999
YMW221U	*MAT**a** lys2-801 ura3-52 his3Δ-200 trp1Δ-63 leu2-1 arp2-2(G19D)::URA3*	Madania *et al.*, 1999
YKT382	*MAT**a** bni1Δ::HIS3MX6*	This study
YKT388	*MAT**a** cla4Δ::KanMX6*	This study
DDY1226	*MATα lys2-801 ura3-52 his3Δ-200 trp1Δ-63 leu2-3,112 cof1-22::LEU2*	A gift from Dr. Drubin
DDY1024	*MAT**a** lys2-801 ura3-52 his3Δ-200 leu2-3,112 ade2-101 ade3 pfy1-116::LEU2*	A gift from Dr. Drubin
DDY949	*MAT**a** ura3-52 his3Δ-200 trp1-1 leu2-3,112 rvs167Δ::TRP1*	A gift from Dr. Drubin
DDY318	*MATα lys2-801 ura3-52 his3Δ-200 trp1Δ-63 leu2Δ-1 sac6Δ::LEU2*	A gift from Dr. Drubin
YKT130	*MAT**a** vrp1Δ::LEU2*	Mochida *et al.*, 2002
YKT218	*MAT**a** sla1Δ::KanMX6*	Mochida *et al.*, 2002
DDY546	*MATα lys2-801 ura3-52 his3Δ-200 leu2-3,112 sla2Δ1::URA3*	A gift from Dr. Drubin
YKT186	*MAT**a** sla2Δ1::URA3*	This study
YKT91	*MAT**a** myo3Δ::TRP1 myo5-1::KanMX6*	This study
YKT93	*MAT**a** myo3Δ::TRP1 myo5-218::KanMX6*	This study
YKT111	*MAT**a** myo3Δ::TRP1 myo5-360::KanMX6*	This study
YKT110	*MAT**a** myo3Δ::TRP1 MYO5::KanMX6*	This study
YKT323	*MAT**a** MYO5-TAP::TRP1*	This study
YKT640	*MAT**a** MYO1-GFP::KanMX6*	This study
YKT641	*MAT**a** MYO1-GFP::KanMX6 she4Δ::HIS3MX6*	This study
YJC1431	*MATα leu2 ura3 his3Δ-200 MYO2-GFP::HIS3*	A gift from Dr. Cooper
YKT520	*MAT**a** MYO2-GFP::HIS3*	This study
YKT524	*MAT**a** MYO2-GFP::HIS3 she4Δ::TRP1*	This study
YKT544	*MAT**a** MYO4-GFP::HIS3MX6*	This study
YKT543	*MAT**a** MYO4-GFP::HIS3MX6 she4Δ::TRP1*	This study

[a] YKT strains, except for YKT550, are in YEF473 background. For YKT strains, only relevant genotypes are described.
[b] These strains are derivatives of L40.

as a substrate (Guarente, 1983). β-Galactosidase activity is expressed in Miller units (Miller, 1972).

Microscopic Observations

Microscopic observations were performed as described previously (Mochida *et al.*, 2002) with some modifications. Briefly, to visualize GFP and the actin cytoskeleton simultaneously, exponentially growing cells were fixed with 3.7% formaldehyde (Wako Pure Chemicals, Osaka, Japan). Fixed cells were stained with 1 μM tetramethylrhodamine isothiocyanate (TRITC)-phalloidin (Sigma-Aldrich, St. Louis, MO). To visualize GFP-tagged proteins, cells were grown to early logarithmic phase, harvested, and resuspended in SD medium, and then cells were observed. To quantify actin cytoskeletal polarity, the number of actin patches in the mother cell of randomly selected small- to medium-budded cells was counted by focusing up and down through the mother cell. Small to medium buds were identified to be no >60% the size of the mother cell. Cells were scored as "polarized" when there were no more than three patches in the mother cell. Observations were performed on an ECLIPSE E800 microscope with either the appropriate fluorescence filter sets or differential interference contrast optics (Nikon Instec, Tokyo, Japan). Observations are based on at least 100 cells viewed. The images presented in this article were acquired using a cooled charge-coupled device camera (C4742-95-12NR; Hamamatsu Photonics, Hamamatsu, Japan) and AQUACOSMOS software (Hamamatsu Photonics).

Isolation of MYO5 Motor Mutants

To isolate mutations in *MYO5* that could bypass the temperature-sensitive growth defect of *she4Δ* cells, we randomly mutagenized the motor region of *MYO5* by a PCR-based method (Cadwell and Joyce, 1992). The mutagenic PCR conditions were as follows: 1 μl of plasmid pKT1004 (0.1 μg/μl) as a template, 1 μl of the forward (5'-TTTTGCCAATGGTGGCAGG-3'; 533 base pairs upstream of the

Table 2. The plasmids used in this study

Plasmid	Characteristics/Reference
pBTM116	DBD$_{LexA}$[a], *TRP1*, 2 μm (Bartel *et al.*, 1993)
pKT1286 (pBTM116-SHE4)	DBD$_{LexA}$-SHE4 (full length), *TRP1*, 2 μm
pKT1287 [pBTM116-SHE4 (1–356)]	DBD$_{LexA}$-SHE4 (1–356 aa), *TRP1*, 2 μm
pBTM116-HA	DBD$_{LexA}$-HA, *TRP1*, 2 μm (Imamura *et al.*, 1997)
pKT1295 [pBTM116-HA-SHE4 (357–789)]	DBD$_{LexA}$-HA-SHE4 (357–789 aa), *TRP1*, 2 μm
pGAD-C1, -C2, and -C3	AD$_{GAL4}$[a], *LEU2*, 2 μm (James *et al.*, 1996)
pKT1279 [pGAD-MYO3 (471–814)]	AD$_{GAL4}$-MYO3 (471–814 aa), *LEU2*, 2 μm; isolated in this study from the yeast genomic library Y2HL-C1 provided by Dr. James
pKT1280 [pGAD-MYO5 (493–739)]	AD$_{GAL4}$-MYO5 (493–739 aa), *LEU2*, 2 μm; isolated in this study from the yeast genomic library Y2HL-C3 provided by Dr. James
pKT1281 [pGAD-MYO3 (471–718)]	AD$_{GAL4}$-MYO3 (471–718 aa), *LEU2*, 2 μm
pKT1282 [pGAD-MYO3 (471–671)]	AD$_{GAL4}$-MYO3 (471–671 aa), *LEU2*, 2 μm
pKT1285 [pGAD-MYO3 (471–572)]	AD$_{GAL4}$-MYO3 (471–572 aa), *LEU2*, 2 μm
pKT1284 [pGAD-MYO3 (555–671)]	AD$_{GAL4}$-MYO3 (555–671 aa), *LEU2*, 2 μm
pKT1006 (pBTM116-HA-MYO3motor)	DBD$_{LexA}$-HA-MYO3 motor (1–718 aa), *TRP1*, 2 μm
pACTII-HK	AD$_{GAL4}$-HA, *LEU2*, 2 μm (Ozaki *et al.*, 1996)
pACTII-HK-ACT1	AD$_{GAL4}$-HA-ACT1, *LEU2*, 2 μm (K. Ozaki-Kuroda and Y. Takai, unpublished)
pRS315	*LEU2, CEN6* (Sikorski and Hieter, 1989)
pKT1004 (pRS315-MYO5)	*MYO5, LEU2, CEN6*
pKT1235 (pRS315-MYO5-GFP)	*MYO5-GFP, LEU2, CEN6*
pKT1403 (pRS315-myo5-1-GFP)	*myo5-1-GFP, LEU2, CEN6*
YEplac195	*URA3*, 2 μm (Gietz and Sugino, 1988)
pKT1294 (YEplac195-SHE4)	*SHE4, URA3*, 2 μm
pKT1330 (YEplac195-MYO5)	*MYO5, URA3*, 2 μm
pKT1331 (YEplac195-MYO5Δmotor)	MYO5Δmotor, *URA3*, 2 μm
pKT1332 [YEplac195-MYO5 (V164I)]	*MYO5* (with V164I substitution), *URA3*, 2 μm
pKT1333 [YEplac195-MYO5 (N168I)]	*MYO5* (with N168I substitution), *URA3*, 2 μm
pKT1334 [YEplac195-MYO5 (N209S)]	*MYO5* (with N209S substitution), *URA3*, 2 μm
pKT1335 [YEplac195-MYO5 (K377M)]	*MYO5* (with K377M substitution), *URA3*, 2 μm
pRS316	*URA3, CEN6* (Sikorski and Hieter, 1989)
pKT1290 (pRS316-SHE4)	*SHE4, URA3, CEN6*
pGEX-4T-1	GST (Amersham Biosciences)
pKT1308 (pGEX-4T-1-SHE4)	GST-SHE4
pKT1386 [pGAD-MYO1 (549–695)]	AD$_{GAL4}$-MYO1 (549–695 aa), *LEU2*, 2 μm
pKT1387 [pGAD-MYO1 (549–648)]	AD$_{GAL4}$-MYO1 (549–648 aa), *LEU2*, 2 μm
pKT1388 [pGAD-MYO2 (530–683)]	AD$_{GAL4}$-MYO2 (530–683 aa), *LEU2*, 2 μm
pKT1389 [pGAD-MYO2 (530–636)]	AD$_{GAL4}$-MYO2 (530–636 aa), *LEU2*, 2 μm
pKT1390 [pGAD-MYO4 (531–678)]	AD$_{GAL4}$-MYO4 (531–678 aa), *LEU2*, 2 μm
pKT1391 [pGAD-MYO4 (531–631)]	AD$_{GAL4}$-MYO4 (531–631 aa), *LEU2*, 2 μm

[a] DBD$_{LexA}$ is the DNA-binding domain of LexA. AD$_{GAL4}$ is the transcriptional activating domain of Gal4p.

start codon) and reverse (5'-TGTTCTGCATTCCTGGTG-3'; 3044 base pairs downstream of the start codon) primers (100 μM each), 10 μl of PCR buffer (10$\times$ stock, Mg^{2+} free), 10 μl of MgCl$_2$ (10$\times$ stock, 25 mM), 10 μl of mutagenic dNTPs mixture (10$\times$ stock: 2 mM dATP, 2 mM dGTP, 10 mM dCTP, and 10 mM dTTP), 1 μl of MnCl$_2$ (50 mM), 1 μl (5 U/μl) of *Taq* (Sigma-Aldrich), and 65 μl of double distilled H$_2$O. PCR was carried out as follows: 94°C, 4 min → 94°C, 1 min; 45°C, 1 min; 72°C, 4 min for 30 cycles → 72°C, 10 min → 4°C. The ~3.6-kbp PCR-amplified fragment was cleaned by ethanol precipitation. The mutagenized PCR products were mixed with an equal amount of pKT1331 plasmid, which was linearized by restriction enzyme digestion. This mixture of DNA was introduced into strain YKT275 to allow homologous recombination between the PCR products and the linearized plasmid, and the transformants were plated on YPDA. After incubation at 37°C for 2 d, the resulting colonies were recovered on SDA-Ura plates at 25°C and then rechecked for growth on YPDA plate at 37°C. From 3.6 $\times$ 10^5 initial transformants, 122 mutants were isolated. Of these, 10 plasmids were rescued and reintroduced into YKT275 to confirm the suppressor phenotype. These plasmids were sequenced. Each plasmid con-

tained more than two mutations. The mutations responsible for suppressor activity were determined by site-directed mutagenesis of pKT1330 by using a QuickChange site-directed mutagenesis kit (Stratagene, La Jolla, CA).

Fluid-Phase Endocytosis

Lucifer yellow-carbohydrazide (LY; Sigma-Aldrich) accumulation analysis was performed as described previously (Dulic *et al.*, 1991). Lucifer yellow uptake was carried out for 30 min at 25°C. Samples were observed by fluorescence microscopy as described above.

In Vitro Binding Assay of Myo5p-TAP with GST-She4p

Recombinant She4p was expressed as a GST-fusion protein in *E. coli* DH5α and purified with glutathione Sepharose beads (Amersham Biosciences, Piscataway, NJ), according to the manufacturer's instructions. Preparation of Myo5p-TAP was carried out as described previously (Rigaut *et al.*, 1999) with some modifications. Briefly,

YKT323 cells were grown at 25°C in 1000 ml of YPDA medium to $OD_{600} = 2.0$ and lysed by two passages in a French pressure cell at 1000 psi. After dialysis, the extracts were applied to IgG Sepharose 6 Fast Flow (Amersham Biosciences). After washing with IPP150 (10 mM Tris-Cl pH 8.0, 150 mM NaCl, 0.1% Nonidet P-40), the immobilized Myo5p-TAP was used in an in vitro binding assay. According to the densitometry of SYPRO orange (Molecular Probes, Eugene, OR)-stained bands on SDS-PAGE gel by using LAS-1000 luminescent image analyzer (Fuji Photo Film, Tokyo, Japan), ~1.5 μg of Myo5p-TAP was bound to 10 μl of IgG Sepharose. SYPRO orange staining was carried out according to manufacturer's instructions. Binary mixtures were prepared by adding GST-She4p (final 0.25 μM) to 10 μl of the Myo5p-TAP-bound IgG Sepharose, which was suspended in 100 μl of IPP150. GST-She4p was added to unbound IgG Sepharose as a negative control. Mixtures were incubated for 30 min at 4 or 30°C and then on ice for 10 min, before being washed intensively with IPP150. Protein complexes were subjected to SDS-PAGE, followed by staining with SYPRO orange. The amount of GST-She4p bound to Myo5p-TAP was quantified by densitometry as described above.

RESULTS

Type I Myosins, Myo3p/Myo5p Interact with She4p

To identify proteins that bind She4p and that thereby might be involved in endocytosis, regulation of the actin cytoskeleton, or development of cell polarity, we performed a two-hybrid screen by using full-length She4p as bait. Multiple clones that encode the type I myosins, Myo3p/Myo5p, were identified. One of these encoded Myo5p amino acids 493–739, and another encoded Myo3p amino acids 471–814 (Figure 1A). Interestingly, these She4p-interacting regions overlapped with the respective motor domains. Because Myo3/5p are involved in the uptake step of endocytosis and polarization of the actin cytoskeleton (Geli and Riezman, 1996; Goodson et al., 1996), we focused further analysis on the interaction between She4p and Myo3/5p.

We sought to determine the region of Myo3p required for interaction with She4p. Testing various truncated fragments of Myo3p for the interaction with full-length She4p, we found that a segment consisting of amino acids 471–572 of Myo3p, which is included in the motor domain, was sufficient for this interaction (Figure 1A). Chicken skeletal muscle myosin (type II) has been well studied and its three-dimensional structure has been resolved (Rayment et al., 1993a). Recently, the three-dimensional structure of Dictyostelium discoideum myosin-IE revealed that the core structural elements and topology of the type I myosin motor are essentially identical to those of the type II (Kollmar et al., 2002). When the amino acid sequence of the Myo3p motor domain is aligned with that of chicken skeletal muscle myosin, the She4p-interacting segment of Myo3p corresponds to amino acids 527–631 of chicken skeletal muscle myosin (Cope and Hodge, 2000), a segment that contains three of the four putative actin contact surfaces (Sellers, 1999; see Figure 8A). Two of these (residues 529–558 and 567–578 of chicken skeletal muscle myosin) are located within the lower 50-kDa subdomain and the other (residues 626–647 of chicken skeletal muscle myosin) is referred to loop2 (Sellers, 1999). Thus, the She4p-interacting segment is in the motor domain and overlaps with putative Myo3p actin-binding regions.

The myosin-binding segment of She4p was also determined by the yeast two-hybrid system. Truncated fragments of She4p were fused to the LexA DNA-binding domain and
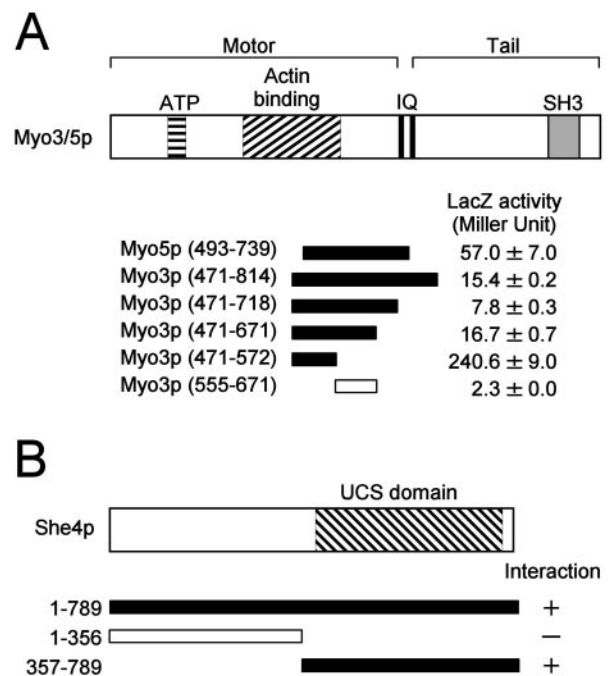

Figure 1. Two-hybrid interactions between She4p and Myo3/5p. DNA fragments encoding various regions of She4p and Myo3/5p were cloned into pBTM (LexA DNA-binding domain plasmids) and pGAD (*GAL4* transcriptional activating domain plasmids) vectors, respectively. The resultant plasmids were introduced into L40 cells. The interactions between She4p and Myo3/5p were examined qualitatively by histidine auxotrophy and quantitatively by β-galactosidase activity assay. The numbers in parentheses represent amino acid positions. Closed bars and open bars stand for His+ and His−, respectively. β-galactosidase (LacZ) activity represents the average and SD for two independent transformants. (A) Interactions between She4p (full length) and various regions of Myo3/5p. ATP, putative ATP-binding domain; IQ, IQ motifs; SH3, Src homology 3 domain. (B) Interactions between various regions of She4p and Myo3p (471–572).

were examined for interaction with Myo3p. She4p was found to bind Myo3/5p through its conserved UCS domain (Figure 1B).

She4p Has Positive Effects on the Interaction between the Myo3p Motor and Act1p

Because She4p-interacting segment of Myo3/5p motor domain overlaps with its actin-binding region, we examined whether She4p affects the myosin motor-actin interaction. The two-hybrid system potentially detects the interaction with F-actin: some F-actin–binding proteins such as Sac6p (fimbrin) give positive interaction with Act1p (yeast actin) in the two-hybrid system (Amberg, unpublished data). We could detect the two-hybrid interaction between the Myo3p motor domain and Act1p, and observed a strong inhibition of reporter transcription in the *she4Δ* strain (Figure 2A). This effect was specific for the Myo3p motor, because the interaction between Act1p and other actin-binding proteins such as Pfy1p (profilin) and Bni1p/She5p (formin) could be detected in the *she4Δ* reporter strain (our unpublished data).
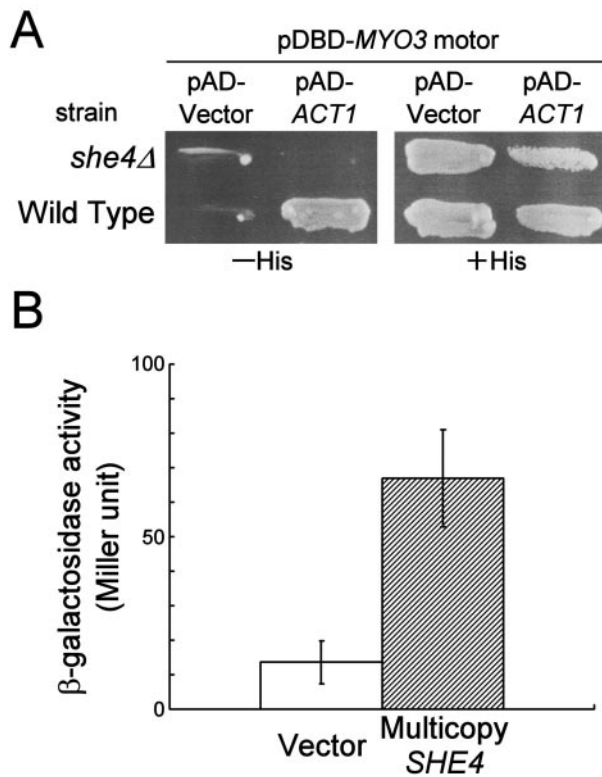
A

B

Figure 2. Effects of *SHE4* disruption or overexpression on the two-hybrid interactions between Myo3p motor and Act1p. (A) L40 (wild-type) and YKT550 (*she4Δ*) cells were transformed with pKT1006 (pDBD-*MYO3* motor) and either pACTII-HK-ACT1 (pAD-*ACT1*) or pACTII-HK (pAD-Vector), and the interaction between the motor domain of Myo3p and Act1p was examined qualitatively by histidine auxotrophy. (B) TAT7 cells containing pKT1006 were transformed simultaneously with pACTII-HK-ACT1 and either pKT1294 (multicopy *SHE4*) or YEplac195 (vector). The interaction between the motor domain of Myo3p and Act1p was examined quantitatively by β-galactosidase activity assay. Bar graph shows the average and SD for five independent transformants.

On the other hand, overexpression of *SHE4* in the wild-type reporter strain enhanced reporter transcription (Figure 2B).

She4p Is Required for Proper Localization of Myo5p

Myo3/5p shows highly polarized localization to patch-like structures enriched in the bud and the cell division site, and these patches partially colocalize with actin cortical patches (Goodson *et al.*, 1996; Anderson *et al.*, 1998). Given the possible role of She4p in proper Myo3/5p function, we questioned whether She4p was required for localization of Myo3/5p to the actin patches. To address this issue, we analyzed the localization pattern of GFP-tagged Myo5p (Myo5p-GFP), expressed under the control of its own promoter in *she4Δ* cells. Disruption of *SHE4* was not associated with significant changes in expression level of Myo5p-GFP as determined by immunoblot analysis by using an anti-GFP antibody (our unpublished data). In wild-type cells, Myo5p-GFP was localized to patch-like structure predominantly existing in the bud and cell division site, and these Myo5p-

patches colocalized with cortical actin patches as reported previously (Goodson *et al.*, 1996; Anderson *et al.*, 1998; Figure 3A). In >99% of *she4Δ* cells, the cortical actin patches lost their polarity (Wendland *et al.*, 1996; Figures 3A and 6C), and Myo5p-GFP diffused throughout the cytosol (Figure 3A). These results indicate that the assembly and/or maintenance of Myo5p in patch-like structures require She4p. Because She4p interacts with the motor domain of Myo3/5p, we examined whether the motor domain is required for proper localization of Myo5p. The temperature-sensitive *myo5-1* mutant has the E472K amino acid substitution, which mimics the E511K substitution of *myo2-66* (Geli and Riezman, 1996). These glutamic acid residues are located in the putative actin-interacting region within the motor domain and, consistent with this, Myo2-66p shows a decreased affinity to actin filaments even in the absence of ATP (Reck-Peterson *et al.*, 2001). Because the She4p-interacting segment of Myo3/5p (amino acids 471–572 in Myo3p) is near this glutamic acid residue, we determined the localization of GFP-tagged Myo5-1p at elevated temperature. In >90% of cells, mainly cytosolic staining and minor cortical punctate staining was observed, and cortical actin patches lost their polarity (Figure 3B). This localization pattern of Myo5-1p-GFP was very similar to that of Myo5p-GFP in *she4Δ* cells. Interestingly, similar results have been reported in *Candida albicans*: amino acid substitution at a putative phosphorylation site by a PAK-like kinase in the motor domain of type I myosin causes its mainly cytosolic localization and depolarization of cortical actin patches (Oberholzer *et al.*, 2002). Our results suggest that mislocalization of Myo5p and concomitant depolarization of cortical actin patches in *she4Δ* cells are caused by dysfunction of the motor domain of Myo3/5p.

We next examined the localization of chromosomally GFP-tagged She4p. This She4p-GFP is functional, because the *SHE4-GFP* strain demonstrated normal polarized localization of cortical actin patches and wild-type growth rate at 37°C (our unpublished data). In contrast to highly polarized localization of Myo5p-GFP, She4p-GFP showed diffuse cytosolic localization (Figure 3C). Similar result has been reported using indirect immunofluorescence study for Myc-tagged She4p (Takizawa and Vale, 2000). Thus, She4p does not seem to colocalize with Myo3/5p, suggesting that She4p and Myo3/5p do not form a stable complex. Rng3p, a UCS protein in *S. pombe*, also shows cytosolic localization (Wong *et al.*, 2000).

Genetic Interactions between *SHE4* and Actin-related Genes and *MYO5*

We examined the genetic interaction of the *she4Δ* mutation with mutations of genes involved in the regulation of the actin cytoskeleton, including *abp1Δ*, *aip1Δ*, *arp2-1*, *arp2-2*, *bni1Δ*, *cla4Δ*, *cof1-22*, *pfy1-116*, *rvs167Δ*, *sac6Δ*, *vrp1Δ*, *sla1Δ*, and *sla2Δ*. The *she4Δ* mutant was crossed with each mutant, and the resulting diploid was sporulated and dissected for tetrad analysis. The growth characteristics of the resulting double mutants were determined at 25°C. The *vrp1Δ*, *arp2-1*, *arp2-2*, and *sla1Δ* mutations exhibited a poor growth phenotype at 25°C when combined with the *she4Δ* mutation, whereas the other double mutants showed little or no reduced growth at 25°C (Figure 4). Vrp1p and the Arp2/3 complex physically interact with the Myo3/5p tail and are
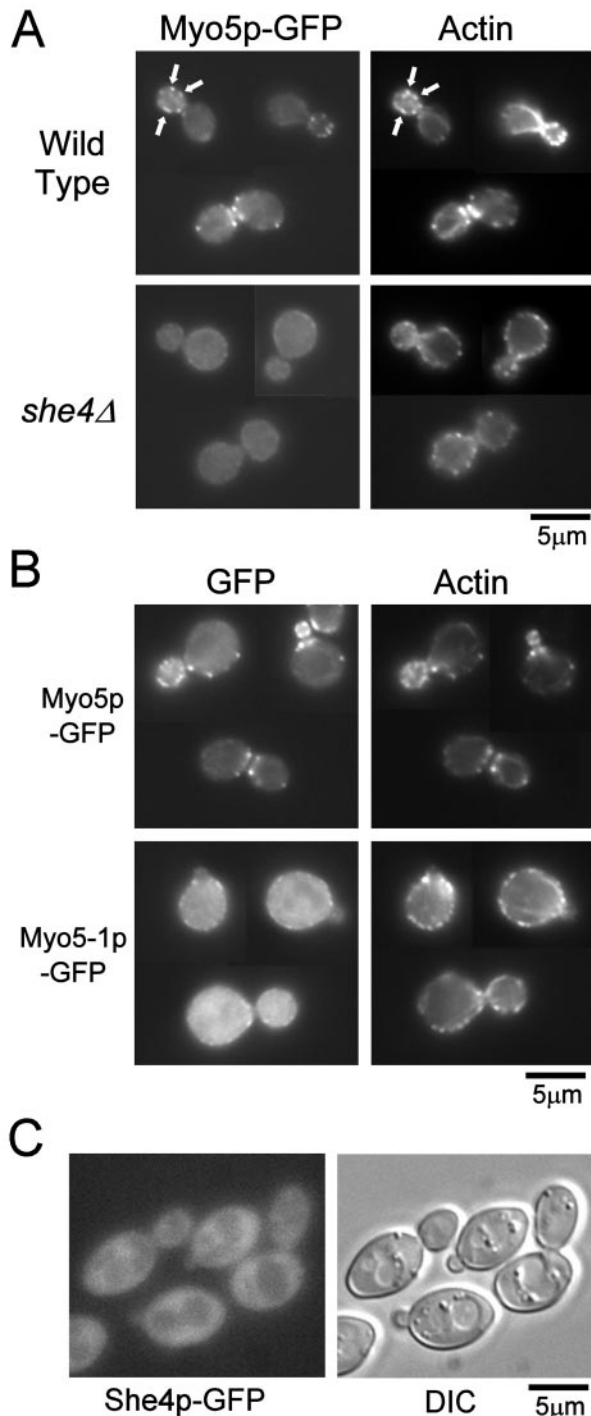
Figure 3. She4p is required for proper localization of Myo5p-GFP and F-actin. (A) Localization of Myo5p-GFP in *she4*Δ cells. Myo5p-GFP expressing cells, YKT159 (wild-type) and YKT288 (*she4*Δ) were grown at 25°C, fixed and stained with TRITC-phalloidin. Localization of Myo5p and F-actin was visualized with a GFP band pass filter (Myo5p-GFP) and a TRITC filter (actin). For each observation, the same exposure and processing parameters were used. Arrows indicate examples of colocalization of Myo5p-GFP and actin patches. (B) Localization of Myo5-1p-GFP. YKT114 cells were trans-

involved in activation of actin polymerization (Evangelista *et al.*, 2000; Geli *et al.*, 2000; Lechler *et al.*, 2000). Consistently, it has been reported that both *arp2-33* and *arc40-40*, mutations in genes encoding subunits of the Arp2/3 actin-nucleating complex, exhibited synthetic lethal interactions with *she4*Δ mutation in systematic genetic analysis (Tong *et al.*, 2001). It is likely that impaired Myo3/5p motor function due to lack of She4p exacerbates the growth defects caused by impaired Myo3/5p-tail–dependent actin polymerization.

Because the *myo5-1* mutation possesses its amino acid substitution (E472K) close to the She4p-interacting segment of the Myo3/5p (amino acids 471–572 in Myo3p), we checked for genetic interaction between *she4*Δ and *myo5-1*. However, the *she4*Δ *myo3*Δ *myo5-1* triple mutant strain was viable and showed no obvious synthetic growth defect compared with a strain containing *she4*Δ single or *myo3*Δ *myo5-1* double mutation (Figure 4A). Interestingly, overexpression of *SHE4* inhibited the growth of *myo5-1* cells at 35°C, a permissive temperature for the *myo5-1* mutant (Figure 5). The *SHE4* overexpression did not inhibit the growth of temperature-sensitive *myo5-218* and *myo5-360* cells with mutations in the tail domain (Figure 5), consistent with the result that She4p binds to Myo3/5p through its motor domain.

Novel Point Mutations in MYO5 Motor Bypass the Requirement of She4p

To further substantiate the role of She4p on Myo3/5p function, we attempted to isolate suppressor *MYO5* mutants that bypass the requirement of She4p. We performed random mutagenesis on the motor region of *MYO5* and screened for mutants that could suppress the temperature-sensitive growth defect of *she4*Δ cells. To enhance the suppression capability, the mutant Myo5ps were expressed from a multicopy plasmid. We identified four amino acid substitutions, V164I, N168I, N209S, and K377M, that could suppress temperature-sensitive growth of *she4*Δ cells (Figure 6A), and surprisingly each of these mutants were able to do so even when carried on low copy vectors (our unpublished data). Because the four mutant plasmids could support the growth of *myo3*Δ *myo5*Δ double mutant cells to an extent similar to that of wild-type at both 25 and 37°C (our unpublished data), these mutations are not likely to have a severe impact on the structure or function of the Myo5p motor. Interestingly, mapping of the locations of these amino acid substitutions on the three-dimensional structure of chicken skeletal muscle myosin (Rayment *et al.*, 1993a) revealed that all substitutions locate inside the cleft separating the upper and the lower 50-kDa subdomains (Figure 6B). This cleft is proposed to open upon ATP-binding and close after hydrolysis, and the open and closed states are coupled with the weak and strong actin-binding states, respectively (Rayment *et al.*, 1993b). These results suggest that a modulation of the actin-
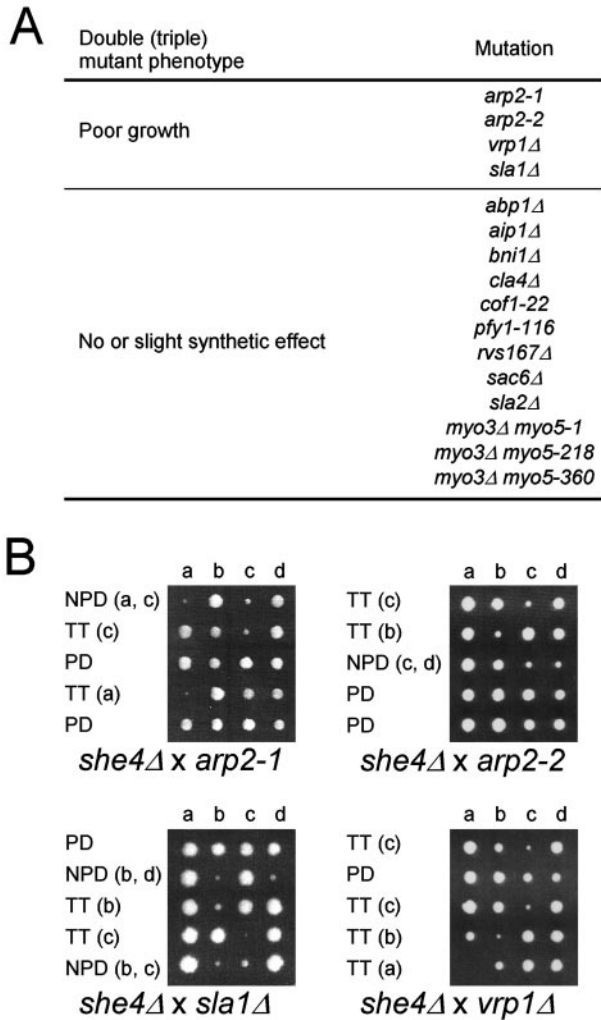
formed with plasmids, pKT1235 (Myo5p-GFP) or pKT1403 (Myo5-1p-GFP). Cells were grown in SD-Leu liquid medium at 25°C, incubated at 37°C for 1 h, fixed, stained, and observed as described in A. (C) Localization of She4p-GFP. She4p-GFP–expressing cells, YKT274, were grown at 25°C, and She4p-GFP was visualized using a GFP band pass filter (She4p-GFP) or differential interference contrast optics (DIC). Bars, 5 μm.

Figure 4. Genetic interactions between *SHE4* and actin-related genes and *MYO5*. (A) Summary of genetic interactions. Each mutant strain was crossed with *she4*Δ (YKT275 or YKT276), and resultant diploid cells were sporulated and dissected for tetrad analysis. The growth characteristics of the resulting double or triple mutants were determined at 25°C. The mutant strains used were YMW211U (*arp2-1*), YMW221U (*arp2-2*), YKT130 (*vrp1*Δ), YKT218 (*sla1*Δ), DDY322 (*abp1*Δ), DDY1520 (*aip1*Δ), YKT382 (*bni1*Δ), YKT388 (*cla4*Δ), DDY1226 (*cof1-22*), DDY1024 (*pfy1-116*), DDY949 (*rvs167*Δ), DDY318 (*sac6*Δ), YKT186 (*sla2*Δ), YKT91 (*myo3*Δ *myo5-1*), YKT93 (*myo3*Δ *myo5-218*), and YKT111 (*myo3*Δ *myo5-360*). (B) Genetic interactions of *arp2-1, arp2-2, sla1*Δ, and *vrp1*Δ with *she4*Δ mutation. Diploid cells obtained from an indicated cross were sporulated, dissected, and grown at 25°C for 3–4 d before being photographed. Colonies were then replica plated to determine the segregation of the marked mutant alleles. Tetrad genotype (TT, tetratype; PD, parental ditype; and NPD; nonparental ditype) is indicated, and the identity of the double mutant spore(s) is shown in parentheses.

binding activities of Myo3/5p may be able to bypass the requirement of She4p for growth at elevated temperatures.

Because type I myosins are involved in polarization of the actin cytoskeleton and endocytosis (Geli and Riezman, 1996; Goodson *et al.*, 1996), we examined effects of these mutated
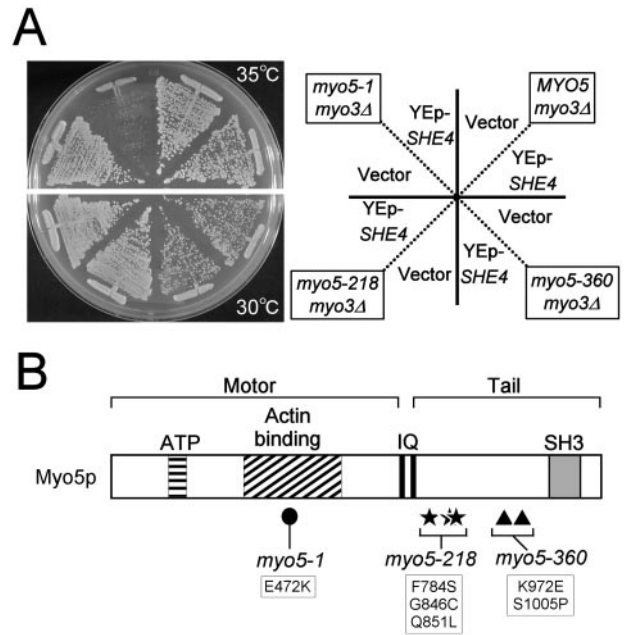

Figure 5. *SHE4* overexpression exacerbates the temperature-sensitive growth defect of the *myo5* motor mutant. (A) YKT91 (*myo5-1*), YKT93 (*myo5-218*), YKT111 (*myo5-360*), and YKT110 (*MYO5*) cells were transformed with pKT1294 (YEp-*SHE4*) or YEplac195 (vector). Transformants were streaked on SDA-Ura plates and incubated for 3 d at 30°C (*myo5-218* and *myo5-360*) or 35°C (*myo5-1* and *MYO5*). (B) The domain structure of Myo5p and the amino acid substitution(s) of *myo5-1* (closed circle), *myo5-218* (stars), and *myo5-360* (triangles) are depicted. ATP, putative ATP-binding domain; IQ, IQ motifs; SH3, Src homology 3 domain.

Myo5ps on actin cytoskeleton and endocytosis in the *she4*Δ mutant. To evaluate effects on distribution of the actin cytoskeleton, we counted the number of actin patches in the mother of small- to medium-budded cells. Whereas *she4*Δ cells with empty plasmid had completely depolarized actin patches (more than three patches in the mother cell; see MATERIALS AND METHODS), *she4*Δ cells with *MYO5*(V164I), *MYO5*(N168I), and *MYO5*(K377M) showed well-polarized distribution of actin patches at a similar level to cells with wild-type *SHE4* (Figure 6C), indicating that mutations in the *MYO5* motor region can suppress depolarization of actin cytoskeleton of *she4*Δ cells. Fluid-phase endocytosis was assessed by uptake of LY. *she4*Δ cells were defective in LY uptake at 25°C (Figure 6D), but all of the *MYO5* mutants restored accumulation of LY in vacuoles (Figure 6D; our unpublished data). These results strongly suggest that defects of *she4*Δ cells in growth at elevated temperatures, actin polarization, and endocytosis are due to dysfunctions of type I myosins.

She4p Interacts with Myo5p in a Temperature-dependent Manner

Our results strongly suggest that She4p plays an important role in the proper functioning of type I myosins through its interaction with their motor domains. It was reported that *C. elegans* UNC-45, which functions as a molecular chaperone for the

Figure 6. Novel dominant point mutations in the *MYO5* motor region can bypass the requirement of She4p. (A) Effects on the temperature-sensitive growth defect of *she4Δ* cells. Plasmids pKT1332 (V164I), pKT1333 (N168I), pKT1334 (N209S), pKT1335 (K377M), pKT1330 (wild-type), and YEplac195 (vector) were introduced into YKT275 cells. Transformants were selected on SDA-Ura plates and streaked on YPDA plates. The plates were incubated for 2 d at 25°C and 37°C. (B) Three-dimensional structure of chicken skeletal muscle myosin S1 (the Protein Data Bank code, 2MYS). Residues corresponding to V164, N168, N209, and K377 of the yeast Myo5p (I222, N226, D264, and K431 of chicken skeletal muscle myosin S1, respectively; Cope and Hodge, 2000) are represented in space-filling format. These residues are located inside the cleft, which extends from the ATP-binding pocket to the actin-binding site and separate the upper and the lower 50-kDa subdomains. This picture was generated using RasMol (Sayle and Milner-White, 1995). (C) Effects on polarized localization of cortical actin patches in *she4Δ* cells. Plasmids YEplac195 (vector), pKT1330 [*MYO5* (WT)], pKT1332 (V164I), pKT1333 (N168I), pKT1334 (N209S), pKT1335 (K377M), and pKT1290 (*SHE4*) were introduced into YKT275 cells. Transformants were grown in SDA-Ura liquid media at 25°C, fixed, and stained with TRITC-phalloidin. Top panels show localization of F-actin of *she4Δ* cells with plasmid pKT1332 [*MYO5* (V164I)] or pKT1290 (*SHE4*). Bar, 5 μm. The bar graph shows the percentage of polarized cell (no more than three patches in the mother cell;

see MATERIALS AND METHODS). (D) Effects on fluid-phase endocytosis defect of *she4Δ* cells. pKT1334 (N209S), pKT1330 (WT), and YEplac195 (vector) were introduced into YKT275. Cells grown in SDA-Ura at 25°C were incubated with lucifer yellow at 25°C for an additional 30 min. Accumulation of lucifer yellow in the vacuole was visualized using an fluorescein isothiocyanate band pass filter (LY). The same exposure and processing parameters were used for comparison. Bar, 5 μm.
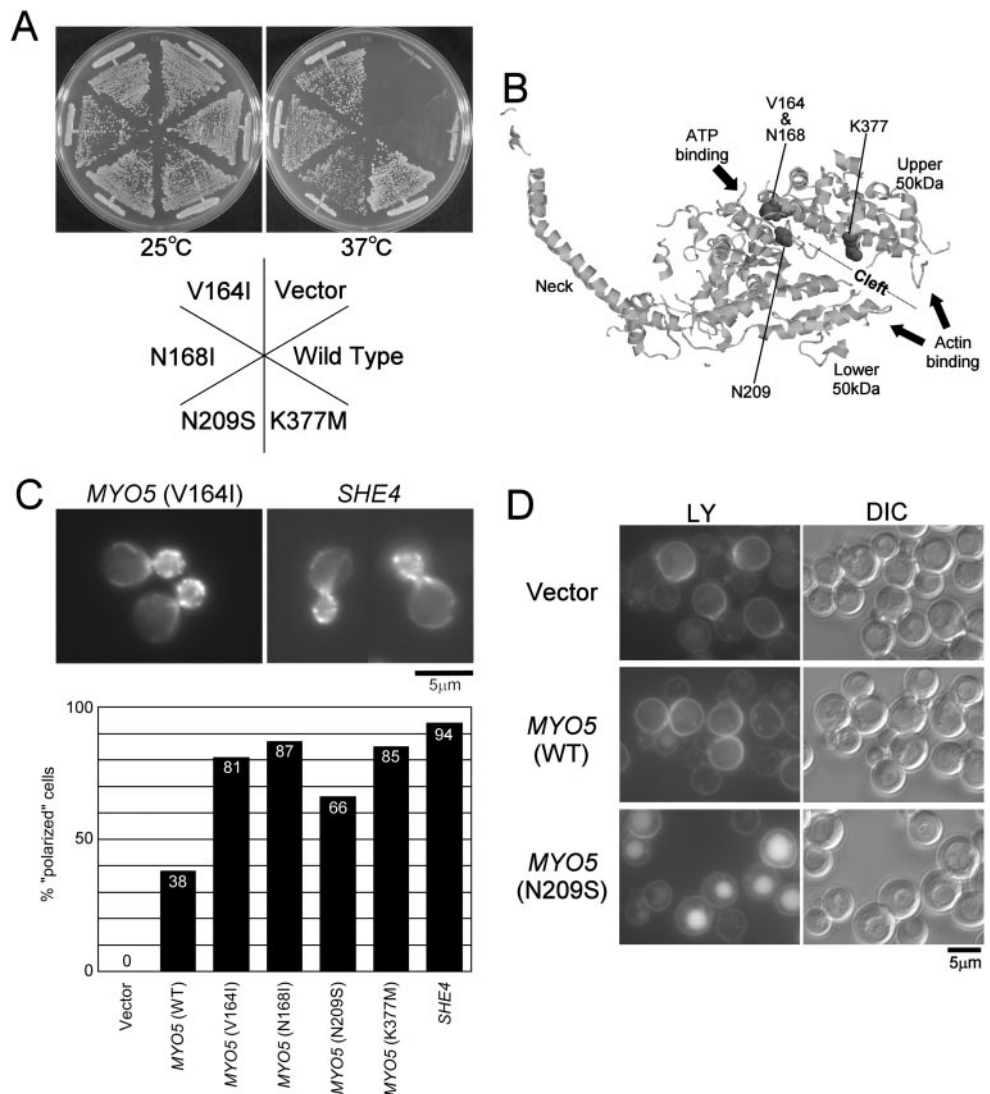
muscle (type II) myosin motor, interacts with the myosin motor in a temperature-dependent manner (Barral *et al.*, 2002). Elevated temperature is required in vitro for the well-studied chaperone, Hsp90 to form complexes with its substrates (Scherrer *et al.*, 1990). Thus, we examined whether She4p interacts with Myo5p in a temperature-dependent manner. The interaction between TAP-tagged Myo5p (Myo5p-TAP), which was bound to IgG beads, and bacterially expressed full-length She4p fused to glutathione *S*-transferase (GST) was examined at 4 or 30°C. Although only a small amount of She4p was collected with Myo5p-TAP at 4°C, the yield was significantly increased at 30°C (Figure 7). The amount of GST-She4p bound to Myo5p-TAP at 30°C was 3.3 times greater than that at 4°C. These results are similar to those observed in the UNC-45-myosin binding experiment.
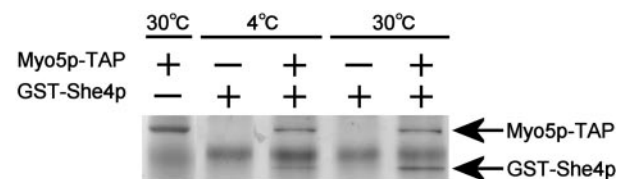

Figure 7. She4p interacts with Myo5p in a temperature-dependent manner. Myo5p-TAP from YKT323 lysate was adsorbed to IgG Sepharose. GST-She4p was purified from bacterial lysate. IgG Sepharose with or without Myo5p-TAP was incubated with GST-She4p at 4 or 30°C. The IgG Sepharose was collected, and bound proteins were analyzed by SDS-PAGE and SYPRO orange staining. The result shown is a representative of four experiments.
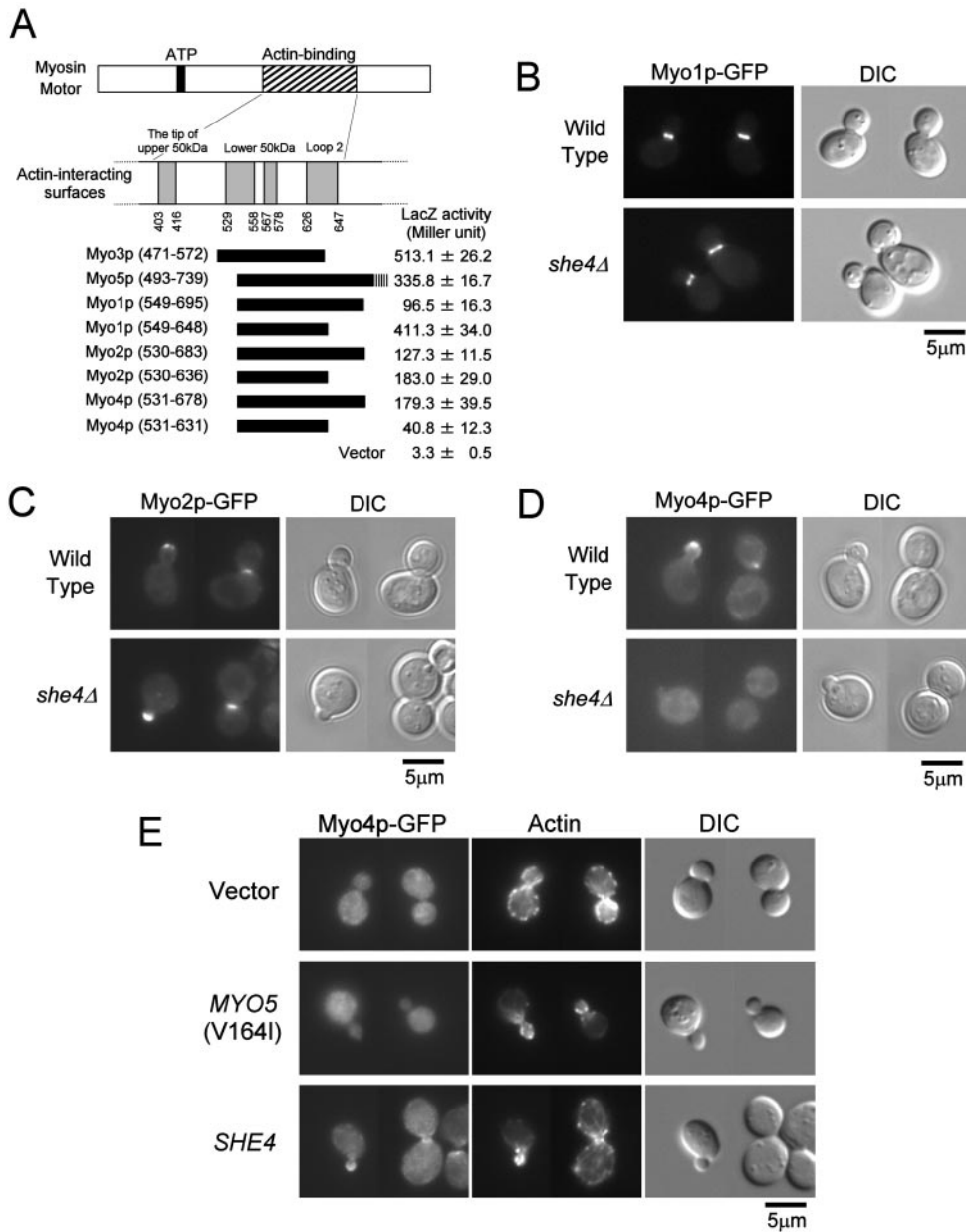
Figure 8. She4p interacts with type II and type V myosins and is required for proper localization of Myo4p. (A) Two-hybrid interactions between She4p and myosins. DNA fragments encoding Myo1p, Myo2p, and Myo4p were cloned into pGAD vectors. The resultant plasmids were introduced into L40 cells carrying pKT1295. The interaction between the UCS domain of She4p and myosins were examined quantitatively by β-galactosidase activity assay. The myosin motor regions used in the experiment were represented schematically. The numbers below actin-binding surfaces and in parentheses represent amino acid positions in chicken skeletal muscle myosin and each yeast myosin, respectively. β-Galactosidase (LacZ) activity represents the average and SD for three independent transformants. (B) Localization of Myo1p-GFP in *she4∆* cells. Myo1p-GFP–expressing cells of YKT640 (wild-type) and YKT641 (*she4∆*) were exponentially grown at 25°C. Myo1p-GFP was visualized using a GFP band pass filter (Myo1p-GFP). The same exposure and processing parameters were used for comparison. Bar, 5 μm. (C) Localization of Myo2p-GFP in *she4∆* cells. YKT520 (wild-type) and YKT524 (*she4∆*) were observed as described in B. Bar, 5 μm. (D) Localization of Myo4p-GFP in *she4∆* cells. YKT544 (wild-type) and YKT543 (*she4∆*) were observed as described in B. Bar, 5 μm. (E) Delocalization of Myo4p-GFP in *she4∆* mutant is not due to depolarization of the actin cytoskeleton. Myo4p-GFP–expressing cells, YKT543, were transformed with YEplac195 (vector), pKT1332 [*MYO5* (V164I)], or pKT1290 (*SHE4*). Transformants were exponentially grown in SDA-Ura at 25°C, fixed, and stained with TRITC-phalloidin. Localization of Myo4p-GFP and F-actin was visualized with a GFP band pass filter (Myo4p-GFP) and a TRITC filter (actin), respectively. For each observation, the same exposure and processing parameters were used. Bar, 5 μm.

She4p Also Interacts with Type II and Type V Myosins and Is Required for Proper Localization of Myo4p

Because the motor domains of the myosin family are highly conserved, it is possible that She4p interacts with and functions for other types of myosins. First, to test their interactions, we performed the two-hybrid assay between C-terminal half (UCS domain) of She4p and segments of Myo1p, Myo2p, and Myo4p, which are approximately equivalent to She4p-interacting segment of Myo3/5p. It was revealed that She4p also interacts with the other yeast myosins, Myo1p, Myo2p, and Myo4p (Figure 8A). Next, we examined whether She4p is

required for localization of Myo1p, Myo2p, and Myo4p. Myo1p-GFP localized normally in *she4∆* cells at the bud neck in >90% of budding cells (Bi *et al.*, 1998; Lippincott and Li, 1998; Figure 8B). Myo2p-GFP normally localized in *she4∆* cells at the bud tip in >90% of budding cells and at the bud neck in large-budded cells as in wild-type cells (Brockerhoff *et al.*, 1994; Lillie and Brown, 1994; Karpova *et al.*, 2000; Figure 8C). In contrast, Myo4p-GFP in >99% of *she4∆* cells diffused uniformly throughout the cytosol (Figure 8D). In wild-type cells, Myo4p-GFP localized at the bud tip in >90% of budding cells and at the bud neck in large-budded cells as reported previ-

ously (Jansen *et al.*, 1996; Munchow *et al.*, 1999; Takizawa and Vale, 2000; Figure 8D). These results indicate that She4p also shows two-hybrid interactions with type V myosins and is required for the proper localization of Myo4p. The requirement of She4p for Myo4p localization is consistent with the hypothesis that "she" phenotype (Ash1p in the mother and daughter nuclei) of *she4* mutant is due to dysfunction of Myo4p. However, another explanation is that delocalization of Myo4p results from depolarization of the actin cytoskeleton. To test this possibility, we analyzed localization of Myo4p-GFP in *she4Δ* cells, where a *MYO5* suppressor mutant restored the actin cytoskeletal polarity. *she4Δ* cells (>99%) still showed delocalization of Myo4p-GFP, even when their actin cytoskeletal polarity was restored by a *MYO5* suppressor mutant (Figure 8E). Thus, delocalization of Myo4p does not seem to be secondary effects of the depolarized actin cytoskeleton.

DISCUSSION

In this article, we show that the UCS domain of She4p physically interacts with the motor domain of type I myosins Myo3/5p. The isolation of *MYO5* suppressor mutations that bypass the growth, endocytic, and actin cytoskeletal defects of the *she4Δ* mutant firmly established that She4p functions through the interactions with Myo3/5p.

The She4p-interacting segment of Myo3/5p overlaps with the putative actin-interacting segment, and the two-hybrid data suggest that She4p plays an important role in the motor-actin interaction. Consistent with this, colocalization of Myo5p and F-actin is disrupted in *she4Δ* cells. Moreover, dominant suppressor mutations in the *MYO5* motor are located in a region that may affect the actin-binding activity of Myo3/5p. These results suggest that one possible function of She4p is to regulate the interaction between the Myo3/5p motor and F-actin. We attempted to examine the biochemical properties of Myo5p in *she4Δ* cells, but we were not able to perform an actin-pelleting assay for Myo5p using *she4Δ* cell lysate, because a significant amount of Myo5p was pelleted independently of F-actin (our unpublished data).

Because the interaction between Myo5p-TAP and GST-She4p is temperature dependent like that between myosin and UNC-45, which has an activity of molecular chaperone for myosin motor (Barral *et al.*, 2002), She4p may also play a role as a molecular chaperone for Myo3/5p. Molecular chaperones promote productive protein folding by preventing off-pathway folding reactions, which lead to protein aggregation (Johnson and Craig, 1997). Actin-independent pelleting of Myo5p-TAP (stated above) could be interpreted as aggregation due to a loss of chaperone activity in the *she4Δ* mutant. Because the localization pattern of She4p is mainly cytosolic, She4p is likely to associate transiently with Myo3/5p or Myo4p, for example, immediately after myosin synthesis or after denaturation caused by stress. Because GST-She4p forms a complex with Myo5p-TAP in vitro, there might be a factor such as a cochaperone, which promotes efficient release of Myo5p form She4p. The idea that She4p functions as a molecular chaperone does not contradict our findings. The mutant Myo5ps, which bypass the requirement of She4p, may have the ability to fold by themselves, or may be more stable at elevated temperatures than wild-type Myo5p. The toxicity of *SHE4* overexpression in *myo5-1* strains could be explained if She4p interferes with actin–myosin motor interaction by binding to Myo5-1p at their

actin-binding regions without correction of their incomplete three-dimensional structure. Consistently, although She4p demonstrated two-hybrid interactions with Myo5-1p, overexpression of *SHE4* did not suppress the impaired two-hybrid interaction between Act1p and Myo3–1p (E472K), which possesses an amino acid substitution analogous to that of Myo5–1p (our unpublished data). Although we have not demonstrated that She4p functions as a molecular chaperone for Myo3/5p, if this is the case, She4p is not absolutely required for proper folding of Myo3/5p, because the growth defect of the *she4Δ* mutant was less severe than those of the *myo3Δ myo5Δ* double mutant (our unpublished data).

UNC-45 in *C. elegans* and Rng3p in *S. pombe*, well-studied UCS domain-containing proteins, are implicated in the functions of type II myosins. Unc-45 is proposed to act as a molecular chaperone for myosin motor (Barral *et al.*, 2002). Rng3p colocalizes with a specific mutant protein of the type II myosin Myo2p (Wong *et al.*, 2000), and we detected the interaction between Rng3p and the motor domain of Myo2p by the two-hybrid assay (our unpublished data). Consistent with this, we also showed that She4p interacts with a type II myosin, Myo1p. In addition, She4p interacted with type V myosins, Myo2p, and Myo4p in the two-hybrid system. Therefore, She4p interacts with all of the yeast myosins. However, the degree of requirement of She4p for their proper functioning varies between each myosin. Because *she4* and *myo4* mutant share the she phenotype and Myo4p is delocalized in the *she4* mutant, She4p is most likely required for proper function of Myo4p. In contrast, She4p does not seem to be absolutely required for function of Myo2p, because *she4Δ* cells show normal polarized localization of Myo2p, and do not show any defects in polarized bud growth, which is regulated by Myo2p (our unpublished data). Similarly, *she4Δ* cells show normal bud-neck localization of Myo1p, and do not show any defects in cytokinesis, which is regulated by Myo1p (our unpublished data). There may be another type of functionally redundant protein that interacts with motor domain of Myo2p and Myo1p in *S. cerevisiae*. Based on the assumption that She4p functions as a molecular chaperone, another explanation is that Myo2p and Myo1p may have relatively high efficiency of self-folding.

Our results that She4p interacts with the motor domain of Myo4p and is required for proper localization of Myo4p strongly suggest that She4p also acts on Myo4p in a manner similar to the action of She4p on Myo3p and Myo5p. To further substantiate this possibility, we constructed mutant Myo4ps with N208I and K412M substitutions, which correspond to N168I and K377M in Myo5p, respectively. However, neither *MYO4(N208I)* nor *MYO4(K412M)* suppressed she phenotype of *she4Δ* cells (our unpublished data). This result may suggest that She4p possesses another function in polarized localization of *ASH1* mRNA, in addition to correct folding or regulation of the motor domain of Myo4p. Interestingly, overexpression of the C-terminal half (UCS domain) of She4p was sufficient for suppression of temperature-sensitive growth defect of *she4Δ* cells, but full-length She4p was required for suppression of she phenotype (our unpublished data). The NH_2-terminal half of She4p, which is less conserved than C-terminal UCS domain among the UCS proteins, may have this specific function in polarized localization of *ASH1* mRNA.

ACKNOWLEDGMENTS

Note added in proof: R. P. Jansen's group has also reported that She4p is required for class I and class V myosin function. [Wesche, S., Arnold, M., and Jansen, R.P. (2003). The UCS domain protein She4p binds to myosin motor domains and is essential for class I and class V myosin function. Curr. Biol. *13*, 715–724.]

REFERENCES

Adams, A.E., and Pringle, J.R. (1984). Relationship of actin and tubulin distribution to bud growth in wild-type and morphogenetic-mutant *Saccharomyces cerevisiae*. J. Cell Biol. *98*, 934–945.

Agatep, R., Kirkpatrick, R.D., Parchaliuk, D.L., Woods, R.A., and Gietz, R.D. (1998). Transformation of *Saccharomyces cerevisiae* by the lithium acetate/single-stranded carrier DNA/polyethylene glycol (LiAc/ss-DNA/PEG) protocol. Technical Tips Online. Available at: http://research.bmn.com/tto. Search for "lithium acetate" from the opening page. Accessed May 2, 2003.

Anderson, B.L., Boldogh, I., Evangelista, M., Boone, C., Greene, L.A., and Pon, L.A. (1998). The Src homology domain 3 (SH3) of a yeast type I myosin, Myo5p, binds to verprolin and is required for targeting to sites of actin polarization. J. Cell Biol. *141*, 1357–1370.

Ao, W., and Pilgrim, D. (2000). Caenorhabditis elegans UNC-45 is a component of muscle thick filaments and colocalizes with myosin heavy chain B, but not myosin heavy chain A. J. Cell Biol. *148*, 375–384.

Balasubramanian, M.K., McCollum, D., Chang, L., Wong, K.C., Naqvi, N.I., He, X., Sazer, S., and Gould, K.L. (1998). Isolation and characterization of new fission yeast cytokinesis mutants. Genetics *149*, 1265–1275.

Barral, J.M., Bauer, C.C., Ortiz, I., and Epstein, H.F. (1998). Unc-45 mutations in *Caenorhabditis elegans* implicate a CRO1/She4p-like domain in myosin assembly. J. Cell Biol. *143*, 1215–1225.

Barral, J.M., Hutagalung, A.H., Brinker, A., Hartl, F.U., and Epstein, H.F. (2002). Role of the myosin assembly protein UNC-45 as a molecular chaperone for myosin. Science *295*, 669–671.

Bartel, P., Chien, C.T., Sternglanz, R., and Fields, S. (1993). Elimination of false positives that arise in using the two-hybrid system. Biotechniques *14*, 920–924.

Berteaux-Lecellier, V., Zickler, D., Debuchy, R., Panvier-Adoutte, A., Thompson-Coffe, C., and Picard, M. (1998). A homologue of the yeast *SHE4* gene is essential for the transition between the syncytial and cellular stages during sexual reproduction of the fungus *Podospora anserina*. EMBO J. *17*, 1248–1258.

Bi, E., Maddox, P., Lew, D.J., Salmon, E.D., McMillan, J.N., Yeh, E., and Pringle, J.R. (1998). Involvement of an actomyosin contractile ring in *Saccharomyces cerevisiae* cytokinesis. J. Cell Biol. *142*, 1301–1312.

Bobola, N., Jansen, R.P., Shin, T.H., and Nasmyth, K. (1996). Asymmetric accumulation of Ash1p in postanaphase nuclei depends on a myosin and restricts yeast mating-type switching to mother cells. Cell *84*, 699–709.

Bohl, F., Kruse, C., Frank, A., Ferring, D., and Jansen, R.P. (2000). She2p, a novel RNA-binding protein tethers *ASH1* mRNA to the Myo4p myosin motor via She3p. EMBO J. *19*, 5514–5524.

Brockerhoff, S.E., Stevens, R.C., and Davis, T.N. (1994). The unconventional myosin, Myo2p, is a calmodulin target at sites of cell growth in *Saccharomyces cerevisiae*. J. Cell Biol. *124*, 315–323.

Brown, S.S. (1997). Myosins in yeast. Curr. Opin. Cell Biol. *9*, 44–48.

Cadwell, R.C., and Joyce, G.F. (1992). Randomization of genes by PCR mutagenesis. PCR Methods Appl. *2*, 28–33.

Cope, M.J., and Hodge, T. (2000). A Multiple Alignment of 139 Myosin Sequences and a Phylogenetic Tree. The Myosin Home Page.Available at: www.mrc-lmb.cam.ac.uk/myosin/myosin.html. Accessed April 23, 2003.

Dulic, V., Egerton, M., Elguindi, I., Raths, S., Singer, B., and Riezman, H. (1991). Yeast endocytosis assays. Methods Enzymol. *194*, 697–710.

Elble, R. (1992). A simple and efficient procedure for transformation of yeasts. Biotechniques *13*, 18–20.

Evangelista, M., Klebl, B.M., Tong, A.H., Webb, B.A., Leeuw, T., Leberer, E., Whiteway, M., Thomas, D.Y., and Boone, C. (2000). A role for myosin-I in actin assembly through interactions with Vrp1p, Bee1p, and the Arp2/3 complex. J. Cell Biol. *148*, 353–362.

Geli, M.I., and Riezman, H. (1996). Role of type I myosins in receptor-mediated endocytosis in yeast. Science *272*, 533–535.

Geli, M.I., and Riezman, H. (1998). Endocytic internalization in yeast and animal cells: similar and different. J. Cell Sci. *111*, 1031–1037.

Geli, M.I., Lombardi, R., Schmelzl, B., and Riezman, H. (2000). An intact SH3 domain is required for myosin I-induced actin polymerization. EMBO J. *19*, 4281–4291.

Gietz, R.D., and Sugino, A. (1988). New yeast-*Escherichia coli* shuttle vectors constructed with *in vitro* mutagenized yeast genes lacking six-base pair restriction sites. Gene *74*, 527–534.

Goodson, H.V., Anderson, B.L., Warrick, H.M., Pon, L.A., and Spudich, J.A. (1996). Synthetic lethality screen identifies a novel yeast myosin I gene (*MYO5*): myosin I proteins are required for polarization of the actin cytoskeleton. J. Cell Biol. *133*, 1277–1291.

Guarente, L. (1983). Yeast promoters and *lacZ* fusions designed to study expression of cloned genes in yeast. Methods Enzymol. *101*, 181–191.

Hollenberg, S.M., Sternglanz, R., Cheng, P.F., and Weintraub, H. (1995). Identification of a new family of tissue-specific basic helix-loop-helix proteins with a two-hybrid system. Mol. Cell. Biol. *15*, 3813–3822.

Imamura, H., Tanaka, K., Hihara, T., Umikawa, M., Kamei, T., Takahashi, K., Sasaki, T., and Takai, Y. (1997). Bni1p and Bnr1p: downstream targets of the Rho family small G-proteins which interact with profilin and regulate actin cytoskeleton in *Saccharomyces cerevisiae*. EMBO J. *16*, 2745–2755.

James, P., Halladay, J., and Craig, E.A. (1996). Genomic libraries and a host strain designed for highly efficient two-hybrid selection in yeast. Genetics *144*, 1425–1436.

Jansen, R.P., Dowzer, C., Michaelis, C., Galova, M., and Nasmyth, K. (1996). Mother cell-specific *HO* expression in budding yeast depends on the unconventional myosin Myo4p and other cytoplasmic proteins. Cell *84*, 687–697.

Johnson, J.L., and Craig, E.A. (1997). Protein folding in vivo: unraveling complex pathways. Cell *90*, 201–204.

Johnston, G.C., Prendergast, J.A., and Singer, R.A. (1991). The *Saccharomyces cerevisiae MYO2* gene encodes an essential myosin for vectorial transport of vesicles. J. Cell Biol. *113*, 539–551.

Karpova, T.S., Reck-Peterson, S.L., Elkind, N.B., Mooseker, M.S., Novick, P.J., and Cooper, J.A. (2000). Role of actin and Myo2p in polarized

secretion and growth of *Saccharomyces cerevisiae.* Mol. Biol. Cell *11*, 1727–1737.

Kilmartin, J.V., and Adams, A.E. (1984). Structural rearrangements of tubulin and actin during the cell cycle of the yeast *Saccharomyces.* J. Cell Biol. *98*, 922–933.

Kollmar, M., Durrwang, U., Kliche, W., Manstein, D.J., and Kull, F.J. (2002). Crystal structure of the motor domain of a class-I myosin. EMBO J. *21*, 2517–2525.

Lechler, T., Shevchenko, A., and Li, R. (2000). Direct involvement of yeast type I myosins in Cdc42-dependent actin polymerization. J. Cell Biol. *148*, 363–373.

Lillie, S.H., and Brown, S.S. (1994). Immunofluorescence localization of the unconventional myosin, Myo2p, and the putative kinesin-related protein, Smy1p, to the same regions of polarized growth in *Saccharomyces cerevisiae.* J. Cell Biol. *125*, 825–842.

Lippincott, J., and Li, R. (1998). Sequential assembly of myosin II, an IQGAP-like protein, and filamentous actin to a ring structure involved in budding yeast cytokinesis. J. Cell Biol., *140*, 355–366.

Long, R.M., Singer, R.H., Meng, X., Gonzalez, I, Nasmyth, K., and Jansen, R.P. (1997). Mating type switching in yeast controlled by asymmetric localization of *ASH1*mRNA. Science *277*, 383–387.

Long, R.M., Gu, W., Lorimer, E., Singer, R.H., and Chartrand, P. (2000). She2p is a novel RNA-binding protein that recruits the Myo4p-She3p complex to *ASH1*mRNA. EMBO J. *19*, 6592–6601.

Longtine, M.S., McKenzie, A.III, Demarini, D.J., Shah, N.G., Wach, A., Brachat, A., Philippsen, P., and Pringle, J.R. (1998). Additional modules for versatile and economical PCR-based gene deletion and modification in *Saccharomyces cerevisiae.* Yeast *14*, 953–961.

Madania, A., Dumoulin, P., Grava, S., Kitamoto, H., Scharer-Brodbeck, C., Soulard, A., Moreau, V., and Winsor, B. (1999). The *Saccharomyces cerevisiae* homologue of human Wiskott-Aldrich syndrome protein Las17p interacts with the Arp2/3 complex. Mol. Biol. Cell *10*, 3521–3538.

Miller, J.H. (1972). Experiments in Molecular Genetics. Cold Spring Harbor, NY: Cold Spring Harbor Laboratory Press.

Mochida, J., Yamamoto, T., Fujimura-Kamada, K., and Tanaka, K. (2002). The novel adaptor protein, Mti1p, and Vrp1p, a homolog of Wiskott-Aldrich syndrome protein-interacting protein (WIP), may antagonistically regulate type I myosins in *Saccharomyces cerevisiae.* Genetics *160*, 923–934.

Mooseker, M.S., and Cheney, R.E. (1995). Unconventional myosins. Annu. Rev. Cell Dev. Biol. *11*, 633–675.

Munchow, S., Sauter, C., and Jansen, R.P. (1999). Association of the class V myosin Myo4p with a localised messenger RNA in budding yeast depends on She proteins. J. Cell Sci. *112*, 1511–1518.

Oberholzer, U., Marcil, A., Leberer, E., Thomas, D.Y., and Whiteway, M. (2002). Myosin I is required for hypha formation in *Candida albicans.* Eukaryot. Cell *1*, 213–228.

Ozaki, K., Tanaka, K., Imamura, H., Hihara, T., Kameyama, T., Nonaka, H., Hirano, H., Matsuura, Y., and Takai, Y. (1996). Rom1p and Rom2p are GDP/GTP exchange proteins (GEPs) for the Rho1p small GTP binding protein in *Saccharomyces cerevisiae.* EMBO J. *15*, 2196–2207.

Pruyne, D., and Bretscher, A. (2000). Polarization of cell growth in yeast. I. Establishment and maintenance of polarity states. J. Cell Sci. *113*, 365–375.

Rayment, I., Rypniewski, W.R., Schmidt-Base, K., Smith, R., Tomchick, D.R., Benning, M.M., Winkelmann, D.A., Wesenberg, G., and Holden, H.M. (1993a). Three-dimensional structure of myosin subfragment-1: a molecular motor. Science *261*, 50–58.

Rayment, I., Holden, H.M., Whittaker, M., Yohn, C.B., Lorenz, M., Holmes, K.C., and Milligan, R.A. (1993b). Structure of the actin-myosin complex and its implications for muscle contraction. Science *261*, 58–65.

Reck-Peterson, S.L., Tyska, M.J., Novick, P.J., and Mooseker, M.S. (2001). The yeast class V myosins, Myo2p and Myo4p, are nonprocessive actin-based motors. J. Cell Biol. *153*, 1121–1126.

Rigaut, G., Shevchenko, A., Rutz, B., Wilm, M., Mann, M., and Seraphin, B. (1999). A generic protein purification method for protein complex characterization and proteome exploration. Nat. Biotechnol. *17*, 1030–1032.

Rodriguez, J.R., and Paterson, B.M. (1990). Yeast myosin heavy chain mutant: maintenance of the cell type specific budding pattern and the normal deposition of chitin and cell wall components requires an intact myosin heavy chain gene. Cell Motil. Cytoskeleton *17*, 301–308.

Sayle, R.A., and Milner-White, E.J. (1995). RASMOL: biomolecular graphics for all. Trends Biochem. Sci. *20*, 374–376.

Scherrer, L.C., Dalman, F.C., Massa, E., Meshinchi, S., and Pratt, W.B. (1990). Structural and functional reconstitution of the glucocorticoid receptor-hsp90 complex. J. Biol. Chem. *265*, 21397–21400.

Schott, D.H., Collins, R.N., and Bretscher, A. (2002). Secretory vesicle transport velocity in living cells depends on the myosin-V lever arm length. J. Cell Biol. *156*, 35–39.

Sellers, J.R. (1999). Myosins, 2nd ed., Oxford, UK: Oxford University Press.

Sherman, F. (1991). Getting started with yeast. Methods Enzymol. *194*, 3–21.

Sikorski, R.S., and Hieter, P. (1989). A system of shuttle vectors and yeast host strains designed for efficient manipulation of DNA in *Saccharomyces cerevisiae.* Genetics *122*, 19–27.

Sil, A., and Herskowitz, I. (1996). Identification of asymmetrically localized determinant, Ash1p, required for lineage-specific transcription of the yeast HO gene. Cell *84*, 711–722.

Takizawa, P.A., Sil, A., Swedlow, J.R., Herskowitz, I., and Vale, R.D. (1997). Actin-dependent localization of an RNA encoding a cell-fate determinant in yeast. Nature *389*, 90–93.

Takizawa, P.A., and Vale, R.D. (2000). The myosin motor, Myo4p, binds Ash1 mRNA via the adapter protein, She3p. Proc. Natl. Acad. Sci. USA *97*, 5273–5278.

Tong, A.H., *et al*. (2001). Systematic genetic analysis with ordered arrays of yeast deletion mutants. Science *294*, 2364–2368.

Venolia, L., and Waterston, R.H. (1990). The *unc-45*gene of *Caenorhabditis elegans* is an essential muscle-affecting gene with maternal expression. Genetics *126*, 345–353.

Watts, F.Z., Shiels, G., and Orr, E. (1987). The yeast *MYO1*gene encoding a myosin-like protein required for cell division. EMBO J. *6*, 3499–3505.

Wendland, B., McCaffery, J.M., Xiao, Q., and Emr, S.D. (1996). A novel fluorescence-activated cell sorter-based screen for yeast endocytosis mutants identifies a yeast homologue of mammalian eps15. J. Cell Biol. *135*, 1485–1500.

Wendland, B., Emr, S.D., and Riezman, H. (1998). Protein traffic in the yeast endocytic and vacuolar protein sorting pathways. Curr. Opin. Cell Biol. *10*, 513–522.

Wong, K.C., Naqvi, N.I., Iino, Y., Yamamoto, M., and Balasubramanian, M.K. (2000). Fission yeast Rng3p: an UCS-domain protein that mediates myosin II assembly during cytokinesis. J. Cell Sci. *113*, 2421–2432.